

$^{39}\text{K}(p, d)^{38}\text{K}$  reaction at  $E_p = 35$  MeV

B. H. Wildenthal and J. A. Rice

*Cyclotron Laboratory\* and Department of Physics, Michigan State University, East Lansing, Michigan 48824*

B. M. Freedom†

*Department of Physics, University of South Carolina, Columbia, South Carolina 29208*

(Received 29 July 1974)

The  $^{39}\text{K}(p, d)^{38}\text{K}$  reaction at  $E_p = 35$  MeV has been used to study the properties of states in  $^{38}\text{K}$  up to an excitation energy of 6 MeV. An experimental resolution of 10 keV (full width at half-maximum) made it possible to detect many heretofore unobserved states. Excitation energies of observed states are determined to an accuracy of 1–4 keV. Angular distributions were measured for many of the transitions, and for these states assignment of  $l_n$  values and extraction of spectroscopic factors is made. The results are compared to previous experiments and to current shell-model calculations.

NUCLEAR REACTIONS  $^{39}\text{K}(p, d)$ ,  $E_p = 35$  MeV; measured  $\sigma(E_d, \theta)$ ; deduced  $Q$  value, excitation energies,  $l_n$  values, and spectroscopic factors for states of  $^{38}\text{K}$ . Natural target.

## I. INTRODUCTION

In the simplest shell-model picture, the lowest energy states of the odd-odd nucleus  $^{38}\text{K}$  should arise from the couplings of two  $d_{3/2}$  holes to  $(J^\pi, T)$  values of  $(3^+, 0)$ ,  $(1^+, 0)$ ,  $(0^+, 1)$ , and  $(2^+, 1)$ . The incorporation of  $s_{1/2}$ -hole excitations is the logical first improvement to this picture; this step taken by Glaudemans, Wiechers, and Brussaard in their pioneering shell-model study of the upper  $s$ - $d$ -shell nuclei.<sup>1</sup> Their results describe successfully many aspects of the low-lying positive-parity states in  $^{38}\text{K}$ . However, much as appears to be the case for the two-*particle* nucleus in the  $s$ - $d$  shell,  $^{18}\text{F}$ , the mixing of the  $d_{3/2}$  and  $d_{5/2}$  orbits may be important even in the lowest few energy levels of  $^{38}\text{K}$ . Several calculations which consider excitations in all three  $s$ - $d$ -shell orbits have been reported,<sup>2–4</sup> and appear to yield still further improvement in the agreement between theory and experiment. There are still significant differences between the results of different specific calculations in the full  $s$ - $d$ -shell space, however, and, even for the lowest few states, lack of complete agreement between any single calculation and the over-all experimental situation. Finally, again in analogy with  $^{18}\text{F}$  and excitations from the  $p$  shell, above the first few states the structure of  $^{38}\text{K}$  cannot be explained in final detail without recourse to excitations from the  $s$ - $d$  shell to the  $f$ - $p$  shell. Some initial investigations along these lines have also been reported.<sup>5,6</sup>

We attempt in the present work to provide an accurate and complete experimental summary of

two aspects of the structure of  $^{38}\text{K}$ . The first of these involves making a catalog of as many of the levels in the low-energy region as possible, and assigning to them precise values of excitation energy. To this end we have measured multiple spectra, using the  $(p, d)$  reaction on  $^{39}\text{K}$ , with a resolution [10 keV, full width at half-maximum (FWHM)] that is at least three times better than that achieved in any of the previous particle-detection work on this nucleus<sup>7,8</sup> and 10 times better than that achieved in previous single-neutron transfer experiments<sup>9–12</sup> leading to  $^{38}\text{K}$ . The second aspect of our study involves obtaining the  $l_n$  values of the neutron transfers which populate these states, and the spectroscopic factors associated with these transfers. These parameters are extracted from angular distributions which were measured into an angle of  $3^\circ$  so as to provide a complete sampling of the  $l_n=0$  strength. We will discuss our results in their relation to the previous experimental situation and with respect to their implications for the current theoretical pictures for this and neighboring nuclei.

## II. EXPERIMENTAL PROCEDURES

Thin ( $\approx 70$   $\mu\text{g}/\text{cm}^2$ ) targets were made by evaporating natural potassium metal (93%  $^{39}\text{K}$ , 7%  $^{41}\text{K}$ ) onto thin carbon backings (30  $\mu\text{g}/\text{cm}^2$ ). These targets were kept under vacuum throughout the experiment and the thicknesses were estimated from the  $(p, d)$  yields and scattering chamber geometry. The targets were bombarded with 35-MeV protons from the Michigan State University cyclotron, and

TABLE I. Optical-model parameters used in the analysis of the  $^{39}\text{K}(p, d)^{38}\text{K}$  data.

Particle	$V_R$ (MeV)	$r_R$ (fm)	$a_R$ (fm)	$W_V$ (MeV)	$r_V$ (fm)	$a_V$ (fm)	$W_{sf}$ (MeV)	$r_{sf}$ (fm)	$a_{sf}$ (fm)	$V_{so}$ (MeV)	$r_{so}$ (fm)	$a_{so}$ (fm)	$r_c$ (fm)
Proton <sup>a</sup>	45.66	1.17	0.75	5.0	1.32	0.53	3.36	1.32	0.53	6.2	1.01	0.75	1.17
Deuteron <sup>b</sup> (FRNL and DFRNL)	87.48-0.35 $E_{c.m.}$	1.25	0.729				13.0	1.25	0.766	6.0	1.25	0.729	1.3
Deuteron <sup>c</sup> (ADIABATIC)	103.79 <sup>d</sup>	1.17	0.779	1.08 <sup>d</sup>	1.29	0.589	17.53 <sup>d</sup>	1.29	0.583	6.2	1.01	0.75	1.17
Neutron bound state	Adjusted to match separation energy	1.24	0.65							$\lambda = 25$			1.24

<sup>a</sup> Reference 13.<sup>b</sup> Reference 27. Averaged parameter Set 1 of Hinterberger *et al.*<sup>c</sup> Reference 32. Neutron and proton parameters from Ref. 13.<sup>d</sup> Values shown are for  $E_x = 0.000$  MeV only;  $Q$  dependence as given in Ref. 13 was used.

reaction products were analyzed in an Enge-type split-pole magnetic spectrograph. Deuteron spectra were obtained both with a single-wire proportional counter and with 25- $\mu\text{m}$ -thick nuclear emulsion plates.

The counter data yielded angular distributions at closely spaced angles from  $3^\circ$  to  $55^\circ$  for the strongly populated levels separated from their neighbors by more than the counter resolution of 50 keV FWHM. The spectrograph acceptance aperture was 0.6 msr for angles less than  $30^\circ$  and 1.4 msr for angles greater than  $30^\circ$ . An appropriate change of the spectrograph magnetic field allowed observa-

tion of protons elastically scattered from potassium in an experimental configuration otherwise identical to that used for the  $(p, d)$  measurements. Data for  $\text{K}(p, p)\text{K}$  were taken at angles from  $35^\circ$  to  $50^\circ$  and the cross-section normalization for the  $(p, d)$  data was taken relative to these elastic cross sections, after an appropriate adjustment of the measured proton yields for the 7%  $^{41}\text{K}$  target contamination. The measured proton elastic scattering intensities were assumed to have the cross sections predicted from an optical model calculation using the Becchetti-Greenlees<sup>13</sup> parameters (see Table I). We estimate an uncertainty of 10%

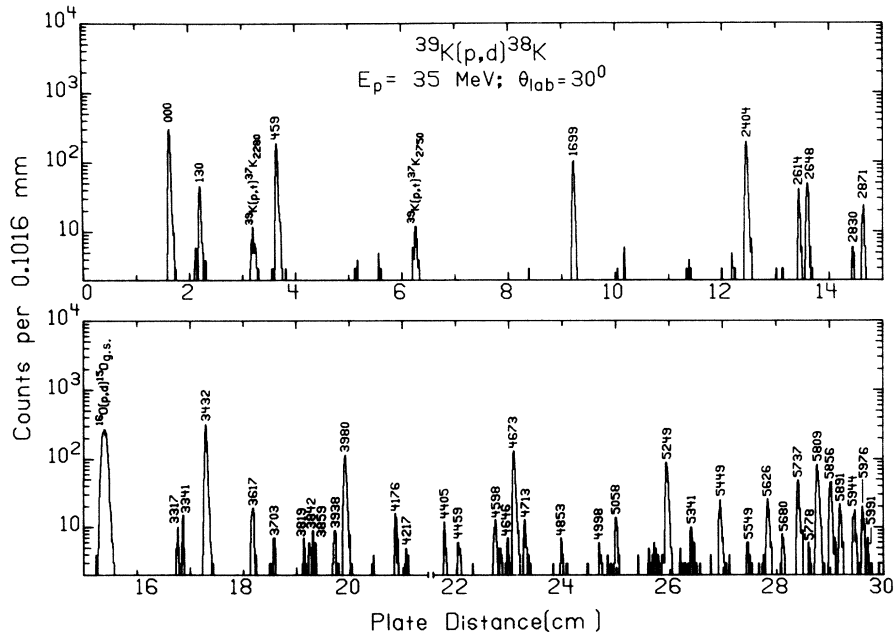


FIG. 1. A spectrum from the  $^{39}\text{K}(p, d)^{38}\text{K}$  reaction, measured at 35 MeV and  $30^\circ$ , as recorded on nuclear emulsion plates. The resolution of the deuteron groups is 10 keV FWHM. All  $^{38}\text{K}$  excitation energy values are from the present work.

in the optical model predictions for this mass and angular range, and an uncorrelated 10% uncertainty in the mechanics of our normalization procedures.

Spectra were also taken with nuclear emulsions at laboratory angles from  $4^\circ$  to  $42^\circ$ . A typical example is shown in Fig. 1. The average resolution obtained for the deuteron groups here was approximately 10 keV FWHM. The spectrograph acceptance apertures were the same as those used for the counter data. Levels in  $^{38}\text{K}$  up to 6 MeV of excitation were recorded. For each angle, the deuteron spectrum up to approximately 4.5 MeV was collected on one 25-cm-long emulsion plate, with the remainder of the deuteron groups and the proton groups from scattering on  $^{12}\text{C}$ ,  $^{16}\text{O}$ , and  $^{39}\text{K}$  falling on a second abutting plate. Relative normalization of all deuteron and proton spectra was accomplished by the use of a NaI monitor detector which recorded protons elastically scattered at  $90^\circ$  to the beam. A beam current integrator was also used to check normalization consistency.

### III. RESULTS

#### A. Excitation energies

Centroids of the deuteron and proton groups which were used in the analysis and assignment of excitation energies were extracted from the spectra recorded with nuclear emulsions at 14, 18, and  $20^\circ$ . The analysis involved the fitting of selected reference peak energies to precisely known values<sup>14-18</sup> via a least-squares iteration of the beam energy, the scattering angle, the small gap between the abutting plates, and the parameters appropriate to a quadratic  $B\rho$  vs focal-plane-distance relationship.<sup>15</sup> The reference peaks chosen (used only at those angles for which they yielded accurate unambiguous centroids) are shown in Table II. In all cases appropriate target-loss corrections were taken into account.

We found it impossible to obtain a good fit to the reference energies if we used the currently quoted<sup>14</sup>  $Q$  value for  $^{39}\text{K}(p,d)^{38}\text{K}$  of  $-10.860 \pm 8$  keV. An equal-weight, minimum  $\chi^2$  fit to all reference peaks was obtained by adjusting this accepted value by +9 keV. This same adjustment was required if all levels from  $^{39}\text{K}(p,d)^{38}\text{K}$  except the ground state were omitted from the calibration data set. The greatest adjustments to the nominal beam energy and scattering angle which the fits required were 8 keV and  $0.2^\circ$ , respectively. These changes are compatible with the accuracy with which we set up the cyclotron beam line and the scattering chamber-spectrograph geometry.

The assignment of any given level to  $^{38}\text{K}$  was made on the basis of a series of angle-to-angle

TABLE II. States used in the energy calibration for the  $^{39}\text{K}(p,d)^{38}\text{K}$  reaction data.

Reaction	Excitation energy in residual nucleus (keV)
$^{39}\text{K}(p,d)^{38}\text{K}$	Ground state <sup>a</sup>
	459.6 $\pm 1.2$ <sup>b</sup>
	1699.4 $\pm 1.3$ <sup>b</sup>
	2403.8 $\pm 1.2$ <sup>b</sup>
$^{16}\text{O}(p,d)^{15}\text{O}$	2871.0 $\pm 1.2$ <sup>b</sup>
	Ground state <sup>c</sup>
$^{12}\text{C}(p,d)^{11}\text{C}$	Ground state <sup>c</sup>
	1.9992 $\pm 1.0$ <sup>d</sup>
$^{39}\text{K}(p,p)^{39}\text{K}$	Ground state
	2522.7 $\pm 0.3$ <sup>e</sup>
	3019.3 $\pm 0.2$ <sup>e</sup>
$^{16}\text{O}(p,p)^{16}\text{O}$	Ground state
$^{12}\text{C}(p,p)^{12}\text{C}$	Ground state
	4440.0 $\pm 0.5$ <sup>f</sup>

<sup>a</sup> Adjusted as described in text.

<sup>b</sup> Reference 16.

<sup>c</sup> Reference 14.

<sup>d</sup> Reference 15.

<sup>e</sup> Reference 17.

<sup>f</sup> Reference 18.

comparisons of measured excitation energy. A level in  $^{40}\text{K}$  [from  $^{41}\text{K}(p,d)^{40}\text{K}$ ] misidentified at  $14^\circ$  as belonging to  $^{38}\text{K}$  would, at  $20^\circ$ , show a shift in assigned excitation energy of almost 4 keV because of the incorrect assumption made for the target mass. Shifts of this type, easily observed in the present high resolution data, naturally increase for larger angular differences, lighter nuclei, and  $(p,t)$  reactions, allowing the unambiguous assignment of the various particle groups to specific residual nuclei.

The present analysis allowed the assignment of excitation energies to several levels in  $^{40}\text{K}$  which fall close to the lowest few levels of  $^{38}\text{K}$  on the spectrograph focal plane. Two of these levels, to which we make assignments of 2258 and 2575 keV, are quoted from Ge(Li) detector studies of their  $\gamma$  ray decays to have  $E_x = 2260.6 \pm 1.0$  keV and  $2574.7 \pm 1.0$  keV.<sup>19</sup> Since the  $Q$  value for  $^{41}\text{K}(p,d)^{40}\text{K}$  is known ( $-7871.3 \pm 1.4$  keV) to good accuracy<sup>14</sup> and our analysis here indicates that  $Q(^{41}\text{K}(p,d)^{40}\text{K}) - Q(^{39}\text{K}(p,d)^{38}\text{K}) = 2980 \pm 2$  keV, we can assign  $Q(^{39}\text{K}(p,d)^{38}\text{K}) = -10851 \pm 2$  keV either on the basis of this "local" comparison, which is essentially independent of the over-all focal-plane calibration, or on the basis of the systematic calibration over 50 cm of the focal plane as described above.

The excitation energies we assign to levels of  $^{38}\text{K}$  observed in the present study are presented in Table III. Also presented in this table are results of other studies of  $^{38}\text{K}$ .<sup>7-12, 16, 20-22</sup> It can be seen that

TABLE III. Energy levels of  $^{38}\text{K}$  excited in the present investigation of the  $(p, d)$  reaction and in previous studies of other reactions.

$(p, d)^a$	$(d, \alpha, \gamma)^h$	$(d, \alpha, \gamma)^c$	Excitation energy (keV)					
			(H, I., $\gamma$ ) <sup>d</sup> and ( $\beta, \gamma$ ) <sup>e</sup>	$(d, \alpha)^f$	$(d, \alpha)^g$	$(d, t)^h$	$(^3\text{He}, \alpha)^i$	$(^3\text{He}, \alpha)^j$
000	000			000	000	000	000	000
130 ± 1	131.4 ± 1.2		130 <sup>d</sup>	144	119	128	138	13(0)
459 ± 1	459.6 ± 1.2	458.8 ± 1		459	43(0)	456	466	45(0)
1699 ± 2	1699.4 ± 1.3	1698.2 ± 1		1702	169(0)	1704	170(0)	170(0)
2404 ± 2	2403.8 ± 1.2	2401.4 ± 1		2403	241(0)	2405	240(0)	240(0)
2614 ± 2	2614.1 ± 1.4	2612.9 ± 0.4		2624	261(0)			
2648 ± 2	2649.4 ± 1.8	2648.3 ± 0.7	2646 <sup>d</sup>		263(0)	2639	263(0)	264(0)
2830 ± 2	2831.5 ± 1.3	2829.0 ± 1.2			281(0)			
2871 ± 2	2871.0 ± 1.2	2869.9 ± 0.9		2864	284(0)		285(0)	287(0)
	2995 ± 2	2993.2 ± 1.1		3000	297(0)			
					305(0)			
3317 ± 2	3319 ± 2	3314.6 ± 0.8		3327	333(0)			
3341 ± 2	3347 ± 3	3341.5 ± 1.3	3337 <sup>e</sup>					
		3418 ± 2.1	3420 <sup>d</sup>		342(0)			
3432 ± 2	3432 ± 2		3458 <sup>d</sup>	3440	344(0)	3441	342(0)	344(0)
3617 ± 2					360(0)			
	3670 ± 2	3668 ± 1.6			365(0)			
3703 ± 4		3725 ± 1.9		3691	367(0)			
					370(0)			371(0)
3819 ± 3					379(0)			
3842 ± 4					381(0)			
		3848.5 ± 2						
3859 ± 4				3865	383(0)			
3938 ± 3					391(0)			
3980 ± 3				3980	394(0)	3989	397(0)	400(0)
4176 ± 3					414(0)			420(0)
4217 ± 3					418(0)			
4321 ± 4								
4338 ± 4								436(0)
4405 ± 4								
4459 ± 4								450(0)
4598 ± 3								
4646 ± 4								
4673 ± 3						4660	466(0)	467(0)
4713 ± 4								
4853 ± 4								
4998 ± 4								
5058 ± 4								508(0)
5249 ± 5							523(0)	525(0)
5341 ± 5								
5449 ± 4							544(0)	545(0)
5549 ± 6								
5626 ± 4								562(0)
5680 ± 5								
5737 ± 4								
5778 ± 6								
5809 ± 6								578(0)
5856 ± 5								585(0)
5891 ± 5								
5944 ± 5								
5976 ± 5								
5991 ± 5								

<sup>a</sup> Present work.<sup>b</sup> Reference 16.<sup>c</sup> Reference 22.<sup>d</sup> Reference 20.<sup>e</sup> Reference 21 ( $\pm 10$  keV).<sup>f</sup> Reference 7 (quoted to only the nearest 10 keV).<sup>g</sup> Reference 8.<sup>h</sup> Reference 11 ( $\pm 15$  keV).<sup>i</sup> Reference 12 (quoted to only the nearest 10 keV).<sup>j</sup> Reference 9 (quoted to only the nearest 10 keV).

almost all levels of  $^{38}\text{K}$  observed in other reactions are found in the present work. Below 4 MeV excitation there appear to be six levels observed in  $(d, \alpha)^{7,8}$  particle-detection experiments or in  $(d, \alpha)^{16,22}$  and heavy-ion initiated $^{20}$   $\gamma$ -detection experiments which we do not see in the  $(p, d)$  spectra. Correspondences can be established between the 19 levels we do observe in this region and previously reported levels. Of the six levels we do not observe, three are seen by at least two other investigations, while two are reported only by Janecke<sup>9</sup> and one only by Engelbertink.<sup>20</sup> There is reason to think<sup>20</sup> that the 3420 and 3458 keV levels have  $J \geq 5$ , which would be consistent with their being very weakly populated with the  $(p, d)$  reaction. There are no such simple explanations available for our not observing the other four levels. In the 4–5 MeV region of excitation Janecke again reports two or three more levels than we observe, but the discrepancies between his and our energy calibrations make it difficult to unambiguously identify levels in that region.

Of the total of 46 levels below 6 MeV excitation observed in the present study, only 20 had been observed in the various previous studies of single-nucleon transfer reactions leading to  $^{38}\text{K}$ . All of the levels reported in these earlier investigations are observed in the present work.

The assignments for excitation energies made

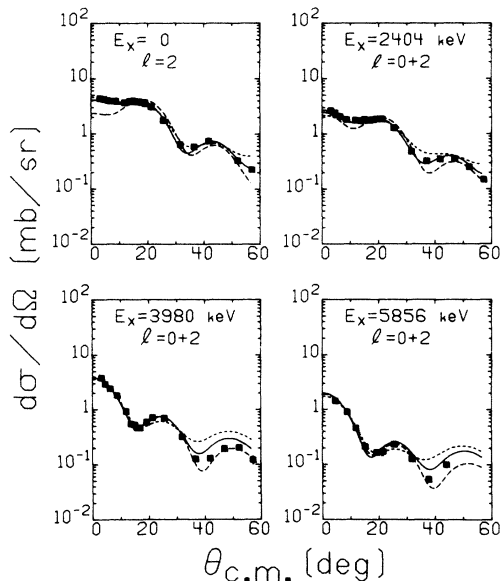


FIG. 2. A comparison of fits to representative angular distribution from the  $^{39}\text{K}(p, d)^{38}\text{K}$  reaction at 35 MeV with the three chosen (see text and Table I) types of DWBA calculations. All fits were performed over the  $3^\circ$  to  $35^\circ$  angular region. The curves are identified by: solid lines, DFRNL; short-dashed lines, FRNL; and long-dashed lines, ADIABATIC.

in the present study agree well with the results of the most precise of the previous investigations.<sup>7, 16, 20–22</sup> The uncertainties quoted for our excitation energies are the estimated probable errors, compounded from fluctuations in peak positions inherent in the scanning of the emulsions, uncertainties in the calibration energies, and uncertainties in the details of the spectrograph calibration. They are consistent with the scatter observed in analyzing several different spectra with several different variations in the way in which the energy-analysis program is applied. Values of the differences in excitation energy between pairs of states up to 1 MeV apart should always be good to 1–2 keV as long as both were populated with reasonable strength.

## B. Angular distributions

### 1. Discussion of distorted-wave Born-approximation calculations

The distorted-wave Born-approximation (DWBA) calculations we discuss here were all made with the code DWUCK.<sup>23</sup> The proton optical model parameters of Ref. 13 were used throughout. Although another set of proton parameters<sup>24</sup> produces discernibly different proton elastic scattering predictions for  $s$ - $d$  shell nuclei at  $E_p = 35$  MeV, the DWBA  $(p, d)$  predictions are quite insensitive to the differences between these two proton potentials.

There is a lack of extensive deuteron elastic

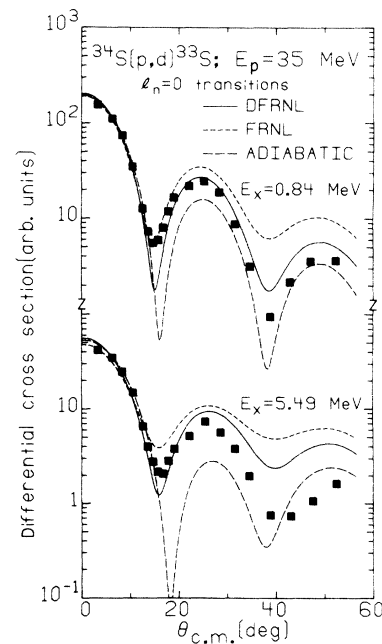


FIG. 3. A comparison of ADIABATIC, FRNL, and DFRNL calculations (see text and Table I) with  $l = 0$  transitions in the  $^{34}\text{S}(p, d)^{33}\text{S}$  reaction at 35 MeV.

scattering data for the mass region of the  $s$ - $d$  shell at energies appropriate to the present experiment. This necessitated an extensive survey of the relevant literature in an attempt to find a suitable set of deuteron optical model parameters. The test of suitability was, of course, the capability of reproducing our observed angular distribution shapes. The criterion for a good  $l=2$  prediction was to match known pure  $l=2$  distributions obtained in the present work and in simultaneously performed measurements of the  $^{35}\text{Cl}(p, d)^{34}\text{Cl}$  reaction.<sup>25</sup> Correspondence to the pure  $l=0$  transitions leading to the 0.842 and 5.49 MeV levels in  $^{33}\text{S}$ , observed<sup>26</sup> via the  $^{34}\text{S}(p, d)^{33}\text{S}$  reaction at  $E_p = 35$  MeV, was used as the criterion for good  $l=0$  DWBA shapes. These "test-case" data are presented in Figs. 2 and 3.

We investigated the efficacy of deuteron potentials proposed by Hinterberger *et al.*,<sup>27</sup> Perey and Perey,<sup>28</sup> Newman *et al.*,<sup>29</sup> Schwandt and Haeberli,<sup>30</sup> and Mermaz *et al.*<sup>31</sup> in both the local zero-range (LZR) and the approximate finite-range non-local (FRNL) versions of the DWBA. The non-locality parameters used for the proton and deuteron channels were the standard<sup>23</sup> values 0.85 and 0.54 fm, respectively. The geometry of the neutron bound-state wave function had the standard Woods-Saxon form,  $r_0 = 1.24$  fm,  $a = 0.65$  fm, and a Thomas spin-orbit term with  $\lambda = 25$ . The depth of the bound-state potential well was always adjusted to match the experimental neutron separation energies corresponding to the various excited states of  $^{38}\text{K}$ . The finite-range parameter for the neutron wave function was 0.621.<sup>23</sup> All calculations were done without any lower cutoff in the radial integration.

In addition, we investigated the "adiabatic" prescription for deuteron-proton transfer reactions, as proposed by Johnson and Soper,<sup>32, 33</sup> and shown to yield good results for reactions on lead,<sup>34</sup>  $f$ - $p$  shell,<sup>33</sup> and oxygen<sup>35, 36</sup> targets and a "density-dependent" damping of the free  $p$ - $n$  interaction as proposed by Freedom *et al.*<sup>37</sup>

When any of the conventional<sup>27-31</sup> deuteron optical model potentials are used, the calculated shapes of the  $l=0$  and  $l=2$  distributions agree much better with our experimental test cases in the FRNL approximation than in the LZR approximation. The best results obtained with any of the various potentials<sup>27-31</sup> appear to be obtained with the "Set 1" values of Hinterberger *et al.*<sup>27</sup> (see Table I). The Hinterberger *et al.* Set 2 and the Newman *et al.* potentials yielded results not too different from those of Set 1.

The critical success of Hinterberger Set 1, relative to potentials of different origins, lies in its correct reproduction of the forward angle ( $\theta_{c.m.} \leq 20^\circ$ )  $l=0$  and  $l=2$  shapes. Its principle failing,

shared by all the others to a greater or lesser extent, is its overestimation of cross sections at larger angles ( $\theta_{c.m.} \geq 30^\circ$ ), a failing which grows more pronounced as the  $Q$  values become more negative (excitation energies get higher, binding energies of transferred neutrons become larger). The quality of agreement between calculation and experiment can be evaluated in Figs. 2 and 3.

Experience led us to expect that both the "adiabatic"<sup>32</sup> and the "density-dependent"<sup>37</sup> alterations to the conventional DWBA procedure would improve the predictions at the larger angles. The adiabatic potential, designed to account for effects resulting from dissociation of the deuteron, is not related to the actual deuteron elastic scattering but is constructed from proton and neutron optical model potentials (taken from Ref. 13 in the present instance) according to a particular prescription.<sup>32, 36</sup> The adiabatic-potential calculations shown were carried out in the LZR approximation.

The "density-dependent damping" of the free  $p$ - $n$  interaction,<sup>37</sup> motivated by a paper by Green,<sup>38</sup> provides an alternate mechanism to reduce DWBA cross sections at larger angles. We use here the damping factor  $F(r) = 1.0 - 1.845\rho(r)^{2/3}$ , where  $\rho(r) = 0.17[1 + \exp(x)]^{-1}$ ,  $x = (r - r_0 A^{1/3})/a$ , and  $r_0$  and  $a$  are the radius and diffusivity of the nuclear matter distribution. The density dependence was studied in conjunction with FRNL calculations which used the Hinterberger *et al.* Set 1 deuteron potential.

We have analyzed our data in detail with the following DWBA calculations (see Table I): (1) the Becchetti-Greenlees<sup>13</sup> proton parameters and Hinterberger *et al.*<sup>27</sup> Set 1 deuteron parameters, using the FRNL approximation (these calculations, henceforth referred to as FRNL, are thus completely orthodox and unadjusted); (2) this same combination of proton and deuteron parameters and computational approximations, but with the addition of the density-dependent damping of the free  $p$ - $n$  interaction, henceforth referred to as DFRNL; and (3) the Becchetti-Greenlees proton parameters and the adiabatic deuteron parameters in the LZR approximation, henceforth referred to as ADIABATIC.

The results of these three types of DWBA calculations are compared with each other and with some of our experimental test data in Figs. 2 and 3. The general characteristics, relative to the experimentally observed  $l_n = 2$  and  $l_n = 0$  transfer distributions, of these calculations are as follows. The FRNL calculations fit the pure  $l_n = 2$   $j = \frac{3}{2}$  observed shapes from  $3^\circ$  out to  $50^\circ$  quite well; the indications are that from  $50^\circ$  on out, the theoretical differential cross sections are too large. For  $l_n = 0$  transitions, the observed shapes are reasonably well reproduced over the second maximum,

but from there on, the theoretical predictions are much too large. In addition, the structure of the theoretical distributions begins to be flattened out for states at higher excitation energies, while the observed shapes seem almost independent of the  $Q$  value involved.

The DFRNL calculations fit the  $l_n=2$  observed shapes essentially perfectly throughout the experimental angular range covered. The agreement with the observed  $l_n=0$  shapes is considerably improved over the FRNL predictions, but cross sections are still somewhat too large beyond  $30^\circ$ , and the undesired trend of shape with  $Q$  value persists.

Finally, the ADIABATIC calculations do not match the forward angle ( $\theta_{c.m.} \leq 15^\circ$ ) behavior observed for the  $l_n=2$  distributions, although for  $\theta_{c.m.} \geq 15^\circ$ , the fits to the data are as good as the FRNL results (but still not as good as the DFRNL results). The differential cross sections predicted for  $\theta_{c.m.} \geq 20^\circ$  for the  $l_n=0$  distributions are indeed lower than those obtained with the FRNL and DFRNL calculations, but over the inclusive region  $3^\circ-40^\circ$ , the agreement with experiment is worse for states at high excitation energy and only comparable for lower energy states.

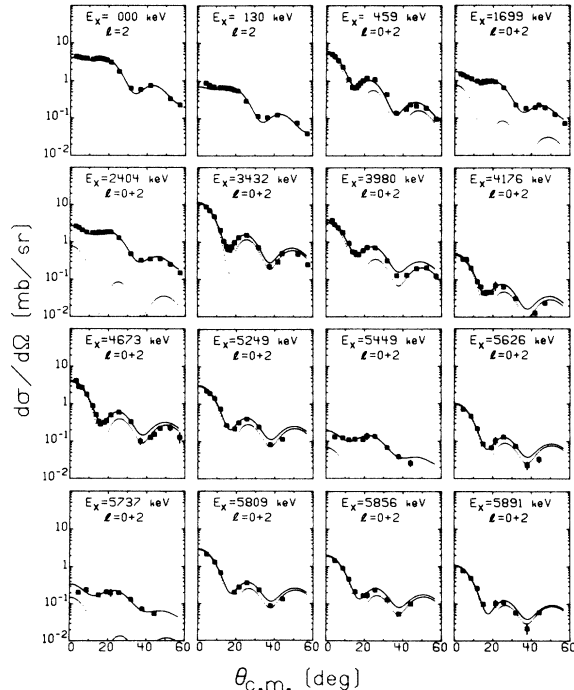


FIG. 4. Experimental angular distributions for the stronger states in  $^{38}\text{K}$ , as observed in the  $^{39}\text{K}(p, d)^{38}\text{K}$  reaction at 35 MeV. The solid curves shown are fits of the DFRNL calculations to the data in the angular range from  $3^\circ$  to  $35^\circ$ . The dotted curves show the amount of the  $l=0$  component in mixed  $l=0-l=2$  distributions.

## 2. Analysis of experimental angular distributions

Our measurements of the angular distributions for states in  $^{38}\text{K}$  populated in the  $^{39}\text{K}(p, d)^{38}\text{K}$  reaction at  $E_p=35$  MeV are presented in Figs. 4 and 5. Some states included in the table of excitation energies are not shown in the figures because they were not observed at enough angles. The solid curves through the data points are fits of the DFRNL calculations described above. Of the 46 levels of  $^{38}\text{K}$  observed in the present investigation, 35 can be assigned at least tentative values for the quantum numbers of the neutron transferred in the process of their formation (see Table IV). 24 levels are assigned pure  $l=2$  or a combination of  $l=2$  and  $l=0$  transfers. The basis for these assignments is typically an excellent and unambiguous fit to the experimental distribution with a mixture of calculated  $l=2$  and  $l=0$  shapes. Most of the transitions having significant  $l=0$  strength are also easily recognized simply on the basis of the unique behavior of the differential cross sections for this type of transfer, which is clearly evident in the  $3^\circ-13^\circ$  portion of our angular distributions.

Assignments of negative-parity  $l$  values ( $l=1$  and 3) could not in general be made with the as-

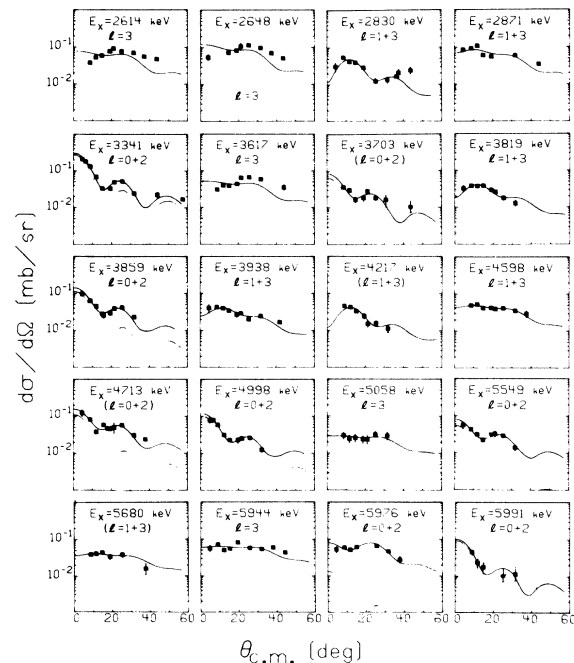


FIG. 5. Experimental angular distributions for the weaker states in  $^{38}\text{K}$ , as observed in the  $^{39}\text{K}(p, d)^{38}\text{K}$  reaction at 35 MeV. The solid curves shown are fits of the DFRNL calculations to the data in the angular range from  $3^\circ$  to  $35^\circ$ . The dotted curves show the amount of the  $l=0$  component in mixed  $l=0-l=2$  distributions.

TABLE IV. Experimental values of  $l$  and  $C^2S_l$ , obtained from the DFRNL analysis for transitions from  $^{39}\text{K}$  to  $^{38}\text{K}$  as observed in the present investigation. The values of  $C^2S$  are normalized so that value for the ground state is 1.75. The assumed  $j$  values are  $\frac{3}{2}$  for  $l=2$ ,  $\frac{3}{2}(n=2)$  for  $l=1$ , and  $\frac{7}{2}$  for  $l=3$ .

$E_x$ (keV)	$J^\pi, T^a$	$l$	$C^2S_l$	$E_x$ (keV)	$J^\pi, T^a$	$l$	$C^2S_l$
000	$3^+, 0$	2	1.75	4271		(1, 3)	0.02, 0.01
130	$0^+, 1$	2	0.31	4598		1, 3	0.005, 0.04
459	$1^+, 0$	0, 2	0.13, 0.32	4673	(1, 2) <sup>+</sup> , 1	0, 2	0.19, 0.25
1699	$1^+, 0$	0, 2	0.02, 0.57	4713		(0, 2)	0.005, 0.05
2404	$2^+, 1$	0, 2	0.03, 1.26	4998		0, 2	0.005, 0.02
2614		3	0.05	5058		3	0.03
2648	(2-5) <sup>-</sup>	3	0.08	5249	(1, 2) <sup>+</sup> , 1	0, 2	0.16, 0.17
2830	(0, 3) <sup>-</sup>	1, 3	0.02, 0.01	5449		0, 2	0.004, 0.15
2871	(0, 3) <sup>-</sup>	1, 3	0.01, 0.05	5549		0, 2	0.003, 0.03
3341	$1^+, 0$	0, 2	0.01, 0.02	5626		0, 2	0.06, 0.05
3432	$2^+, 0$	0, 2	0.43, 0.43	5680		(1, 3)	0.003, 0.04
3617		3	0.04	5737		0, 2	0.009, 0.26
3703		(0, 2)	0.003, 0.02	5809	(1, 2) <sup>+</sup>	0, 2	0.17, 0.16
3819		1, 3	0.01, 0.02	5856	(1, 2) <sup>+</sup>	0, 2	0.11, 0.12
3859		0, 2	0.005, 0.03	5891	(1, 2) <sup>+</sup>	0, 2	0.06, 0.04
3938		1, 3	0.01, 0.02	5944		3	0.08
3980	(2) <sup>+</sup> , 1	0, 2	0.14, 0.42	5976		0, 2	0.001, 0.10
4176		0, 2	0.02, 0.03	5991		0, 2	0.006, 0.01

<sup>a</sup> References 10, 11, 15, 21, 22, and 39.

surance possible for the  $l=0$  and  $l=2$  cases. This was because the experimental distributions were rather featureless (except for a few examples dominated by  $l=1$ ) and because the  $l=3$  calculated shape does not appear to fit the data as well as is the case for  $l=1, 0$ , and 2. As a consequence of these two trends, it is possible in many cases to get as reasonable a fit to the data with a combination of  $l=2$  plus  $l=4$  shapes as it is with  $l=1$  plus  $l=3$  shapes. And, in addition, there is the uncertainty as to whether some of the weakest, flattest distributions observed are even characteristic of a single-step direct transfer. We have assigned negative parity ( $l=3$  and/or 1) to 12 of the levels observed. Many of these assignments, however, are dependent upon an assumption which rules out the possibility of significant  $l=4$  transfer strength.

The fits of the DWBA predictions to the experimental distributions, and the resulting absolute spectroscopic factors, were obtained by minimizing the quantity

$$\chi^2 = \frac{1}{N} \sum_{i=1}^N \left[ \left( 2.29 C^2 S \frac{(d\sigma/d\Omega)(\theta_i)_{i,j, \text{DWUCK}}}{2j+1} - \frac{d\sigma}{d\Omega}(\theta_i)_{\text{exp}} \right) / \Delta\sigma_i \right]^2$$

through the adjustment of the coefficients  $C^2S$ . Here,  $(d\sigma/d\Omega)(\theta_i)_{i,j, \text{DWUCK}}$  are the numbers output from the DWUCK program for angles  $\theta_i$ ,  $(d\sigma/d\Omega) \times (\theta_i)_{\text{exp}}$  are the experimental differential cross

sections and  $\Delta\sigma_i$  are the statistical plus estimated relative systematic errors in the experimental numbers. Values of  $l=0$  plus 2 or 1 plus 3 were used except in special cases where known spin assignments precluded mixing. The number of data points  $N$  included all observations in the angular range  $3^\circ$ – $35^\circ$ . In Table IV we list the excitation energies,  $l_n$ -value assignments, and relative spectroscopic factors for all the states whose angular distributions we considered at least marginally analyzable. The DFRNL DWBA calculations were used in extracting these numbers. The absolute values for the spectroscopic factors can be obtained from the value quoted for the ground state. It should be noted that the absolute values are significantly too large compared to the sum-rule limits.

We carried out the same fitting procedure, again with the DFRNL predictions, including all data points out to  $60^\circ$ . The maximum changes in the resulting spectroscopic factors were 10%. We also carried out the fitting procedure for all distributions, in the  $3^\circ$ – $35^\circ$  angular range, with the FRNL and ADIABATIC DWBA predictions. The DFRNL results are compared to these FRNL and ADIABATIC results and to results of previous experiments and analyses in Table V. Only those states previously observed are included in this table, to keep the size manageable, but these suffice to indicate the trends and scatter of the spectroscopic factors as functions of the details of the

TABLE V. Experimental values of  $C^2S_{lj}$  for the transitions from  $^{39}\text{K}$  to  $^{38}\text{K}$ . The absolute values for the ground state are presented in parentheses. All other values are normalized such that  $C^2S = 1.75$  for the ground state.

$E_x^a$ (keV)	$J^\pi, T$	$l_n$	DFRNL <sup>a</sup>	FRNL <sup>a</sup>	ADIABATIC <sup>a</sup>	$(d, t)^b$	$(^3\text{He}, \alpha)^c$	$(^3\text{He}, \alpha)^d$	$(d, ^3\text{He})$	
000	$3^+, 0$	2	1.75 (3.52)	1.75 (2.51)	1.75 (3.09)	1.75 (1.83)	1.75 (1.83)	1.75 (1.9)	e	f
130	$0^+, 1$	2	0.31	0.31	0.31	0.25	0.32 <sup>g</sup>	0.45	0.25	0.26
459	$1^+, 0$	0	0.13	0.16	0.12	0.10	0.19	0.18		
		2	0.32	0.29	0.33	0.38	0.22	0.27		
1699	$1^+, 0$	0	0.02	0.02	0.04	0.00	0.05	0.07		
		2	0.57	0.53	0.52	0.72	0.56	0.68		
2404	$2^+, 1$	0	0.03	0.00	0.05	0.05	0.27	0.14		
		2	1.26	1.16	1.16	0.98	1.10	1.2	1.25	1.25
2648	$(2-5)^-, 0$	1				0.09	0.02	0.13		
		3	0.05	0.07	0.06		0.08			
3432	$2^+, 0$	0	0.43	0.48	0.35	0.32	0.51	0.51		
		2	0.43	0.14	0.51	0.26	0.07	0.22		
3980	$(1, 2)^+, 1$	0	0.14	0.16	0.13	0.06	0.23	0.23	0.13	0.08
		2	0.42	0.25	0.43	0.48	0.31	0.34		
4673	$(1, 2)^+, 1$	0	0.19	0.20	0.15		0.21	0.29	0.31	0.24
		2	0.25	0.07	0.29	0.49 <sup>h</sup>	0.15	0.12		
5249	$(1, 2)^+, 1$	0	0.16	0.16	0.13		0.18	0.23	0.16	0.12
		2	0.17	0.06	0.22		0.00	0.23		
5449	$(1, 2)^+, 0$	0	0.00	0.00	0.01		0.02	0.02		
		2	0.15	0.11	0.13		0.09			
5809	$(1, 2)^+$	0	0.17	0.16	0.13					
		2	0.16	0.09	0.24					
5856	$(1, 2)^+$	0	0.11	0.11	0.09				0.39	0.32
		2	0.12	0.05	0.16					
5891	$(1, 2)^+$	0	0.06	0.06	0.05					
		2	0.04	0.01	0.07					

<sup>a</sup> Present work; all  $l = 2$  spectroscopic factors for  $d_{3/2}$  transfer.

<sup>b</sup> Reference 11.

<sup>c</sup> Reference 12; radial cutoff = 2.8 fm.

<sup>d</sup> Reference 9;  $E_{^3\text{He}} = 10$  MeV;  $C^2S_{2, 3/2}$  below 2.5 MeV,  $C^2S_{2, 5/2}$  above 2.5 MeV.

<sup>e</sup> Reference 39, multiplied by  $\frac{1}{2}$ .

<sup>f</sup> Reference 40, multiplied by  $\frac{1}{2}$ .

<sup>g</sup>  $C^2S_{0, 1/2} = 0.03$  also reported.

<sup>h</sup>  $l = 3$ .

DWBA calculations.

In the present study, we are not concerned with pursuing the question of the absolute magnitudes of the single-nucleon transfer spectroscopic factors. We are interested primarily in trying to get some measure of the reliability of *relative* spectroscopic factors, both for a particular  $l$  transfer as a function of  $Q$  value (or the separation energy for the picked-up neutron), and also of the relative values for different ( $l=2$  vs  $l=0$ )  $l$  transfers. The latter point reduces, in the limit, to the question of the certainty with which a weak component of one mode of  $l$  transfer can be identified in a transition dominated by the other  $l$ . This, of course, is important beyond just the spectroscopic factor, since the presence of a particular  $l$  has direct implications for the spin of the residual state.

The accuracy with which DWBA calculations reproduce the  $Q$ -dependent effects on over-all cross-

section magnitudes is difficult to pin down. We mentioned in a previous section that details of the angular distributions as a function of  $Q$  value are not well handled in all cases by any of our calculations. The consistency between results obtained with rather different sets of optical model parameters can be examined in Table V. The accuracy (really only the consistency) of the relative magnitudes of the peak cross sections for different  $l$  transfers was also only examined in a comparative sense, and again some of these results can be examined in Table V. The results of these studies, covering not only the three types of DWBA calculations already discussed here in some detail, but also a good many others, indicate that most conventional DWBA formulations for the  $(p, d)$  reaction yield consistent results within the domain of the residual nuclear states studied here. The extent to which these results are "correct" can be

further explored by comparing extracted spectroscopic factors with those obtained from other reactions, as will be done in a following section.

The spectroscopic factors extracted from a fit to (generally) mixed- $l$  angular distributions contain  $Q$ -dependent and  $l$ -dependent uncertainties arising from errors and lack of completeness in the data set, and from failures of the DWBA curves to exactly reproduce the shapes of pure- $l$  distributions, as well as from the more fundamental uncertainties in cross-section trends mentioned above. By measuring the experimental distributions to a forward angle of  $3^\circ$ , we have insured that the  $l=0$  spectroscopic factors are free from the extra uncertainties chronic in many previous studies in which the data covers only the second maximum of the  $l=0$  shape. The intrinsic cross section of the DWBA-calculated  $l=0$  transition at  $3^\circ$  is 20 times the magnitude of the  $l=2$  prediction at its maximum. Hence, our extracted values for  $C^2S(l=0)$  are extremely secure in an experimental sense. That is, there is no way to reproduce the shape of an experimental distribution which has a significant peaking at  $0^\circ$  without putting in essentially the total amount of  $l=0$  strength obtained in our fits. The amount of  $l=0$  admixture in a predominantly  $l=2$  distribution can be given to an accuracy good enough for any meaningful comparison with theoretical predictions. The more interesting question, involving weak to nonexistent  $l=0$  components, concerns the limit at which their presence can definitely be assigned. The better the quality of the data and the better the theoretical fit to pure  $l=2$  shapes, the more stringent a criterion can be employed. We assume that the presence of an  $l=0$  component is unambiguously established if  $C^2S(l=0) \geq 0.005$  as extracted from the present data by the automatic fitting procedure.

The problem of extracting accurate  $l=2$  spectroscopic factors from shapes displaying significant  $l=0$  character is much more difficult than the converse problem. Since the intrinsic magnitudes of the  $l=2$  DWBA cross sections are so much smaller than those of  $l=0$ , and are also relatively unstructured, the amount (and the uncertainty thereof) of  $l=2$  strength in an apparently  $l=0$  experimental shape can be quite significant in terms of nuclear structure predictions. Short of perfect  $l=0$  DWBA predictions and essentially perfect data, this problem seems impossible to overcome. An objective integrating-fit criterion such as we have used is probably not the best approach to extracting  $l=2$  components unless the theoretical  $l=0$  fits are very good. Otherwise it is quite possible that the  $l=2$  strength assigned by the fit serves predominantly to compensate for the principle defects in the  $l=0$  predicted shapes. We

think that the fits of the DFRNL predictions to the data are good enough to justify an automatic non-subjective analysis procedure. However, some of the lack of consistency which crops up in the comparison between spectroscopic factors extracted with the three different calculations obviously arises from deficiencies in the FRNL and ADIABATIC  $l=0$  shapes. And, even in the best cases, it seems the safest course to treat the extracted  $l=2$  spectroscopic factors from " $l=0$ "-type distributions as upper limits.

#### IV. DISCUSSION OF RESULTS

##### A. Comparison with previous experimental results

The agreement between the present results and those of previous nucleon-pickup experiments, presented in Table V, seems quite good. The normalizations applied to the various sets of results are such as to equate the ground state ( $3^+, 0$ )  $l=2$  spectroscopic factor to the sum-rule limit for  $J=3$ . A similar technique is applied to the ( $d, {}^3\text{He}$ )  $l=2$  strengths. With such normalizations we note that the ( $p, d$ ) and ( ${}^3\text{He}, \alpha$ ) spectroscopic factors slightly violate the sum rule for  $J=0^+ T=1$ , while the ( $d, t$ ) and ( $d, {}^3\text{He}$ ) results agree very closely with the limits. The discrepancy is puzzling since the  $Q$  values of this pair of states are so similar.

The general tendency is for the present results to yield smaller  $l=0$  strengths than those reported for ( ${}^3\text{He}, \alpha$ ). The sum of  $l=0$  strength from DFRNL analysis of the present results is 1.61 out of a possible 2.0. The ( $d, {}^3\text{He}$ ) results, for the  $T=1$  states only, exhaust the limit of 2, and the indication is that had the ( ${}^3\text{He}, \alpha$ ) experiments included all states below 6 MeV, they also would account for essentially all of the  $l=0$  strength. Whether these differences are significant or fortuitous is unclear. They do suggest the possibility of a 15% error in the relative  $l=0|l=2$  DWBA strengths as calculated here. Another possibility is that, because we insert (probably) too much  $l=2$  strength when we fit the mixed  $l=0, 2$  experimental distributions, we do not extract quite all of the  $l=0$  strength. This effect could account for no more than  $\sim 0.1$  of the missing 0.4 spectroscopic strength, however.

The main distinctions of the present results are (1) the greater range of excitation studied, (2) the much better experimental resolution and counting statistics, which resulted in many more individual states being discovered and categorized, and (3) the close approach to  $0^\circ$  in the measurement of the angular distributions, which gives a much better look at the dominant part of the  $l=0$  shape. The good fits to the distribution obtained with very straightforward DWBA procedures are sufficient

to give confidence that the spectroscopic factor analysis is on as secure theoretical grounds as the various general ambiguities of the subject presently permit.

### B. Isospin questions

All levels in  $^{38}\text{Ar}$  ( $T = T_z = 1$ ) should have analogs in the spectrum of  $^{38}\text{K}$  which have essentially the same nuclear properties. Experiments<sup>39,40</sup> with the  $^{39}\text{K}(d, ^3\text{He})^{38}\text{Ar}$  reaction show that the  $0^+$  ground state and the  $2^+$  first excited state at 2.167 MeV are excited strongly with  $l=2$  transfer and that the  $2^+$  levels at 3.937, 4.565, and 5.157 and the  $(1, 2)^+$  level at 5.552 MeV<sup>41</sup> are strongly populated by  $l=0$  transfer. It was explained in Ref. 39, before unique spins for the higher states were known, that the spectroscopic factor for states observed in the  $^{39}\text{K}(d, ^3\text{He})^{38}\text{Ar}$  reaction below 6 MeV excitation could be understood in terms of a  $(d_{3/2}^{-1})_{J=3/2}$  model for  $^{39}\text{K}$ ,  $(d_{3/2}^{-2})_{J=0,2}$  wave functions for the ground and first excited states ( $d_{3/2}$  pickup), and  $(d_{3/2}^{-1}s_{1/2}^{-1})_{J=1,2}$  wave functions for the higher-lying  $l=0$  strength. Since only one  $1^+$  and one  $2^+$  state can be formed from the  $s_{1/2}^{-1}-d_{3/2}^{-1}$  coupling and four  $l=0$  states are observed, it is obvious that fragmentation of the  $l=0$  strength into states arising from other configurations occurs. It was argued in Ref. 39 that the fragmentation most probably involved  $2^+$  states (since confirmed), and that the extra two  $2^+$  states had their origins in  $f$ - $p$ -shell configurations rather than in  $d_{5/2}$  hole excitations. The state at 5.55 MeV was suggested to have  $J=1^+$ .

All of these levels strongly excited in  $^{38}\text{Ar}$  should be observed, with similar relative strengths, in the  $^{39}\text{K}(p, d)^{38}\text{K}$  reaction. The analogs of the first five strongly excited  $^{38}\text{Ar}$  levels are observed at 130, 2404, 3980, 4673, and 5249 keV in the present work. Relative to the lowest  $0^+ T=1$  state, the energy shifts of the four excited states in  $^{38}\text{K}$ , relative to  $^{38}\text{Ar}$ , are +107, -87, -22, and -38 keV, respectively.

The analog of the "5.55" (5.552) MeV level of  $^{38}\text{Ar}$  observed in  $(d, ^3\text{He})$  is not clearly identifiable in  $^{38}\text{K}$ . We observe three  $l=0$  transitions in the 5800–5900 keV region in the present experiment. Such a triplet of states would not have been resolved in the  $(d, ^3\text{He})$  study. However, the fact that only one positive-parity level (5.552 MeV) is known to exist in the appropriate energy region of  $^{38}\text{Ar}$  implies that the  $l=0$  transition observed in  $(d, ^3\text{He})$  proceeds to a single ( $T=1$ ) state. Thus two of the three  $l=0$  states we observe in  $^{38}\text{K}$  near 5.85 MeV excitation should have  $T=0$ .

The consistency between the spectroscopic factors extracted from the  $(d, ^3\text{He})$  data and the  $(p, d)$

TABLE VI. Experimental and theoretical values of  $C^2S$  for single neutron pickup from  $^{38}\text{K}$ .

$E_x^a$ (keV)	$J^\pi, T$	$l$	DFRNL <sup>a</sup>	Theory <sup>b</sup>
000	$3^+, 0$	2	, 1.75	, 1.72
130	$0^+, 1$	2	, 0.31	, 0.23
459	$1^+, 0$	0, 2	0.13, 0.32	0.13, 0.40
1699	$1^+, 0$	0, 2	0.02, 0.57	0.04, 0.46
2404	$2^+, 1$	0, 2	0.03, 1.26	0.01, 1.20
3432	$2^+, 0$	0, 2	0.43, 0.43	0.43, 0.15
3980	$(1, 2)^+, 1$	0, 2	0.14, 0.42	
4673	$(1, 2)^+, 1$	0, 2	0.19, 0.25	0.58, 0.05
5249	$(1, 2)^+, 1$	0, 2	0.16, 0.17	
5809	$(1, 2)^+$	0, 2	0.17, 0.16	
5856	$(1, 2)^+$	0, 2	0.11, 0.12	0.37, 0.00 ( $1^+, T=1$ )
5891	$(1, 2)^+$	0, 2	0.06, 0.04	

<sup>a</sup> Present work.

<sup>b</sup> Reference 2.

data can be inspected in Table V. The apparent analogs in  $^{38}\text{K}$  of the first five strongly excited levels in  $^{38}\text{Ar}$  have  $(p, d)$  spectroscopic factors consistent with the  $(d, ^3\text{He})$  values, the largest deviation occurring for the 4.673 MeV state. The failure to find a single state in the 5.85 MeV region of  $^{38}\text{K}$  which has  $l=0$  spectroscopic strength comparable to the  $(1)^+ T=1$  state at the corresponding energy in  $^{38}\text{Ar}$ , would seem to be evidence of almost complete mixing of the  $1^+ T=1$  state with one, and probably both, of the nearby  $T=0$  neighbors discussed above. Indeed, the sum of spectroscopic strength to the three  $^{38}\text{K}$  levels at 5.85 nicely equals the strength of the (presumed) single state in  $^{38}\text{Ar}$ .

It is not possible to establish further isospin assignments in  $^{38}\text{K}$  via correspondences between the  $^{38}\text{K}$  and  $^{38}\text{Ar}$  level schemes because the level densities are high relative to the average Coulomb shifts and because proton pickup data comparable to the present neutron pickup work does not exist.

### C. Comparison of results with structure theory

Pickup spectroscopic factors predicted for  $^{39}\text{K} \rightarrow ^{38}\text{K}$  are compared with the present experimental results in Table VI. The listed theoretical numbers are averages of the predictions derived from the two most successful Hamiltonians studied in Ref. 2, Kuo-type Hamiltonians  $12.5p + ^{17}\text{O}$  and  $11.0h + \text{ASPE}$ . The agreement appears quite impressive, and seems to confirm the essential validity of this particular approach to calculating low-lying positive parity states at the top of the  $s$ - $d$  shell. While the comparison definitely confirms the success of the Kuo matrix elements relative to the other interactions studied, the differences between the individual predictions of these

two interactions were too small to be resolved. Indeed, it would seem to be almost beyond the scope of single-nucleon pickup experiments to meaningfully discriminate between the two sets of wave functions, since the differences which are most significant tend to involve the  $d_{3/2}$ - $d_{5/2}$  mixtures.

The  $s$ - $d$ -shell model of Ref. 2 predicts the first  $(3^+, 0)$ ,  $(0^+, 1)$ , and  $(2^+, 1)$  states of  $A = 38$  to have essentially the simple  $(d_{3/2})^{-2}_{J=3,0, \text{ and } 2}$  wave functions. The ratio of  $l=2$  spectroscopic factors predicted, 1.0/0.14/0.70, is in rather good agreement with the measured 1.0/0.18/0.72, which indicates the general correctness of the above picture. The predictions of Ref. 2 for the lowest two  $(1^+, 0)$  states and for the lowest  $(2^+, 0)$  state are more complex. The  $1^+$  states have quite mixed wave functions; not only are the  $s_{1/2}$ - and  $d_{3/2}$ -hole strengths shared between the two states, but also the shell model theory predicts significant  $d_{5/2}$ -hole strength in the second level. The predictions for the distribution of  $l=0$  and  $l=2$  strength over these states is strikingly well confirmed by the present experimental results. It should further be noted that the predicted and observed  $l=0$  strength for these two states is not nearly the maximum allowed. A  $1^+, 0$  state with significant  $l=0$  strength is predicted<sup>2</sup> in the 5 MeV region. A single state with probable  $T=0$  is not observed in the 5 MeV region with the full predicted  $l=0$  strength, but the existence of several weaker  $l=0$  states in the vicinity suggest that the third  $(1^+, 0)$  state from the  $s$ - $d$ -shell space is fragmented, as was suggested for the case of the higher  $(2^+, 1)$  state.

The properties predicted for the first  $(2^+, 0)$  state are in good agreement with the significant  $l=0$  and  $l=2$  strength observed for the 3432 keV state. For this state and the higher  $T=1$  states with predominant  $l=0$  distributions, we note that the extracted  $l=2$  spectroscopic strengths exceed the predicted values. This is not regarded as significant because of the previously mentioned difficulty in reliably ascertaining  $l=2$  contributions in such contexts. Using our normalization based on the ground state spectroscopic factor, our results indicate a sum of  $l=2$  strength of 4.7. This is of course more than is allowed for  $d_{3/2}$  alone. Some  $d_{5/2}$  strength is predicted in the 0-6 MeV region, and is probably observed. However, the total amount of  $l=2$  strength in the 0-6 MeV region is still more (~10%) than is predicted for both  $d_{3/2}$  and  $d_{5/2}$  and some of this is doubtless is probably an artifact of the automatic extraction procedure we used.

The density of states observed in  $^{38}\text{K}$  above 2.5 MeV is far in excess of what is predicted by the  $d_{5/2}$ - $s_{1/2}$ - $d_{3/2}$  shell model calculations just dis-

cussed, even though these calculations predict the observed apportionment of  $l=0$  and  $l=2$  (mostly, but not all,  $d_{3/2}$ ) strength among the low-lying levels. The drastic fragmentation of the  $l=0$  spectroscopic strengths to "extra"  $T=1$  levels also indicates the existence and significance of states which should arise from  $f$ - $p$ -shell configurations.<sup>39</sup> The number of levels observed above 2.5 MeV is qualitatively in agreement with the results of calculations which include  $f$ - $p$ -shell configurations.<sup>5, 6</sup>

The present spectroscopic factor results contain some evidence bearing on the question of  $f$ - $p$ -shell admixtures for the nuclei involved. The sum of the  $l=3$  strength extracted is 0.47 and the  $l=1$  strength is 0.09. The  $l=3$  value is certainly an upper limit for the region observed since it contains an indeterminate contribution from structureless non-single-step-direct contributions to the weak levels analyzed as  $l=3$ . Perhaps 50% of the recorded strength is a plausible estimate of the true  $l=3$  strength to be apportioned over the presently observed levels. At the minimum there is definite evidence for  $f$ - $p$ -shell components in the  $^{39}\text{K}$  ground state, a result which did not emerge from the  $(d, ^3\text{He})$  results. This result of course implies an inconsistency in our implicit assumption that the full  $d_{3/2}$ - $s_{1/2}$  spectroscopic strength predicted from purely  $s$ - $d$ -shell structure calculations is to be observed for the low-lying levels.

## V. CONCLUSIONS

We have found that the angular distributions of the  $(p, d)$  reaction on  $^{39}\text{K}$  can be successfully analyzed with DWBA calculations which employ the most thoroughly founded proton and deuteron optical-model potentials available. The approximate finite-range, nonlocal DWBA calculations which use such parameters fit both  $l=0$  and  $l=2$  distributions quite well in the  $3^\circ$ - $30^\circ$  range. At larger angles, the calculated cross sections do not drop off as rapidly as do the data. Use of a deuteron potential constructed by folding neutron and proton potentials and use of a density-dependent correction to the free  $p$ - $n$  interaction both serve to improve agreement at larger angles. The density-dependent damping procedure yields the best fits to the present data. Any of these DWBA prescriptions yields stable and theoretically sensible spectroscopic factors if only the  $3^\circ$ - $30^\circ$  data are used.

Many new levels have been observed in the present experiment and the assigned excitation energies are accurate to 1-5 keV. The detailed angular distribution measurements permitted the assignment of a positive parity and spin limits to many of the observed levels, and tentative negative parity to many others. The spectroscopic fac-

tors extracted for the stronger states are, in general, consistent with results of previous neutron and proton pickup experiments. The results for the low-lying positive parity levels provide conclusive verification for the relevant predictions of recent shell-model calculations.

The details of structure observed above 3 MeV

excitations are evidence of extensive effects of  $f$ - $p$ -shell configuration states, but aside from energy level schemes, no predictions from extended ( $s$ - $d$ - $f$ - $p$ ) shell-model calculations are yet available to compare to our results. We observe what appears to be very strong mixing between  $T=0$  and  $T=1$ ,  $J=1^+$  states at 5.85 MeV excitation.

\*Work supported by the National Science Foundation.

†Work supported in part by the Research Corporation.

<sup>1</sup>P. W. M. Glaudemans, G. Wiechers, and P. J. Brussaard, Nucl. Phys. **56**, 548 (1964).

<sup>2</sup>B. H. Wildenthal, E. C. Halbert, J. B. McGrory, and T. T. S. Kuo, Phys. Rev. C **4**, 1266 (1971).

<sup>3</sup>A. E. L. Dieperink and P. J. Brussaard, Nucl. Phys. **A128**, 34 (1969).

<sup>4</sup>R. D. Lawson, reported in H. T. Fortune, N. G. Puttaswamy, and J. L. Yntema, Phys. Rev. **185**, 1546 (1969).

<sup>5</sup>F. C. Erne, Nucl. Phys. **84**, 91 (1966).

<sup>6</sup>G. A. P. Engelbertink and P. W. M. Glaudemans, Nucl. Phys. **A123**, 225 (1969).

<sup>7</sup>I. J. Taylor, Nucl. Phys. **41**, 227 (1963).

<sup>8</sup>J. Janecke, Nucl. Phys. **48**, 129 (1963).

<sup>9</sup>G. Ronsin, M. Vergnes, G. Rotbard, J. Kalifa, and I. Linck, Nucl. Phys. **A187**, 96 (1972).

<sup>10</sup>L. M. Blau, W. P. Alford, D. Cline, and H. E. Gove, Nucl. Phys. **76**, 45 (1965).

<sup>11</sup>Fortune, Puttaswamy, and Yntema (Ref. 4).

<sup>12</sup>J. A. Fenton, T. H. Kruse, N. Williams, M. E. Williams, R. N. Boyd, and W. Savin, Nucl. Phys. **A187**, 123 (1972).

<sup>13</sup>F. D. Becchetti and G. W. Greenlees, Phys. Rev. **182**, 1190 (1969).

<sup>14</sup>A. H. Wapstra and N. B. Gove, Nucl. Data **A9** (Nos. 4-5), 265 (1971).

<sup>15</sup>J. A. Nolen, E. Kashy, I. D. Proctor, and G. Hamilton, unpublished.

<sup>16</sup>W. K. Collins, C. S. C., D. S. Longo, and L. A. Alexander, in University of Notre Dame Nuclear Structure Laboratory Annual Report, 1971.

<sup>17</sup>S. Maripuu, Nucl. Phys. **A151**, 465 (1970).

<sup>18</sup>J. J. Kolata, R. Auble, and A. Galonsky, Phys. Rev. **162**, 957 (1967).

<sup>19</sup>A. N. James, P. R. Alderson, D. C. Bailey, P. E. Carr, J. L. Durell, N. W. Greene, and J. F. Sharpey-Schafer, Nucl. Phys. **A172**, 401 (1971).

<sup>20</sup>G. A. P. Engelbertink, private communication.

<sup>21</sup>A. Gallmann, E. Aslanides, F. Jundt, and E. Jacobs, Phys. Rev. **186**, 1160 (1969).

<sup>22</sup>H. Hasper and P. B. Smith, Phys. Rev. C **8**, 2240 (1973).

<sup>23</sup>P. D. Kunz, unpublished.

<sup>24</sup>M. P. Fricke, E. E. Gross, B. J. Morton, and A. Zucker, Phys. Rev. **156**, 1207 (1967).

<sup>25</sup>J. A. Rice, B. H. Wildenthal, and B. M. Freedom, Bull. Am. Phys. Soc. **17**, 485 (1972); and unpublished.

<sup>26</sup>A. Moalem and B. H. Wildenthal, unpublished.

<sup>27</sup>F. Hinterberger, G. Mairle, V. Schmidt-Rohr, G. J. Wagner, and P. Turek, Nucl. Phys. **A111**, 265 (1968).

<sup>28</sup>C. M. Perey and F. G. Perey, Phys. Rev. **152**, 923 (1966).

<sup>29</sup>E. Newman, L. C. Becker, B. M. Freedom, and J. C. Hiebert, Nucl. Phys. **A100**, 225 (1967).

<sup>30</sup>P. Schwandt and W. Haeberli, Nucl. Phys. **A123**, 401 (1969).

<sup>31</sup>M. C. Mermaz, C. A. Whitten, J. W. Champlin, A. J. Howard, and D. A. Bromley, Phys. Rev. C **4**, 1778 (1971).

<sup>32</sup>R. C. Johnson and P. J. R. Soper, Phys. Rev. C **1**, 976 (1970).

<sup>33</sup>J. D. Harvey and R. C. Johnson, Phys. Rev. C **3**, 636 (1971).

<sup>34</sup>G. R. Satchler, Phys. Rev. C **4**, 1485 (1971).

<sup>35</sup>B. M. Freedom, Phys. Rev. C **5**, 587 (1972).

<sup>36</sup>G. M. McAllen, W. T. Pinkston, and G. R. Satchler, Particles and Nuclei **1**, 412 (1971).

<sup>37</sup>B. M. Freedom, J. L. Snelgrove, and E. Kashy, Phys. Rev. C **1**, 1132 (1970).

<sup>38</sup>A. M. Green, Phys. Lett. **24B**, 384 (1967).

<sup>39</sup>B. H. Wildenthal and E. Newman, Nucl. Phys. **A118**, 347 (1968).

<sup>40</sup>W. S. Gray, P. J. Ellis, T. Wei, R. M. Polichar, and J. Janecke, Nucl. Phys. **A140**, 494 (1970).

<sup>41</sup>P. M. Endt and C. van der Leun, Nucl. Phys. **A214**, 1 (1973).